Denoising and Migration Techniques for Target Identification from Ground Penetrating Radar 2D data; a case study

Olga LOPERA[1,2], Nada MILISAVLJEVIC[1], Bart SCHEERS[1], Benoît MACQ[3]

[1]Signal and Image Centre, Royal Military Academy
30 Av de la renaissance, 1000 Brussels, Belgium

[2]Dept. of Electrical and Electronic Engineering, University of Los Andes
Kr 1 Este 18A-10 Bogota, Colombia

[3]Telecommunications Laboratory, Catholic University of Louvain
2 Place du Levant, 1348 Louvain-la-Neuve, Belgium
olopera@elec.rma.ac.be

Résumé – Le radar de pénétration du sol (GPR) est une technique de télédétection employée pour obtenir l'endroit et la réflectivité spatiaux des objets enterrés. Puisque la plupart des antennes de GPR ne sont pas directives, les signaux dispersés enregistrés par le radar se prolongent au-dessus d'une grande ouverture latérale [1, 2]. Dans cette étude, des algorithmes de débruitage et de migration sont employés pour refocaliser les signaux dispersés de nouveau à leur point d'origine. Les données ont été prises pour différents scénarios. Afin de réaliser la séparation optimale de la signature de la cible de la réponse du soil, techniques de débruitage son utilisées sur les données 2D. La transformée de Hough randomisé est employé pour extraire des informations importantes [3]. Ces informations sont incluses dans un algorithme de migration [4], et la largeur aproximée de l'objet dans la direction du balayage est trouvée. Bien que les résultas sont pormetteurs, les algorithmes doivent toujours être validés dans différentes conditions.

Abstract – Ground-penetrating radar (GPR) is a remote sensing technique used to obtain the spatial location and reflectivity of subsurface objects. Since most GPR antennas have board beam widths, the scattered signals recorded by the radar extend over a large lateral aperture [1, 2]. In this study, denoising and migration algorithms are used to refocus the scattered signals back to their point of origin. The data were collected for different scenarios. In order to achieve optimal separation of the target signatures from the background, denoising techniques are used to filter the signal from the 2D data. The randomized Hough Transform is used to extract relevant features [3]. This extracted information is included in migration algorithms [4], and the approximated width of the target in the scan direction is found. Although the results are promising, algorithms still need to be validated under different conditions.

1 Introduction

Since the WWII, many military conflicts around the world have left more than 100 millions of antipersonnel mines (APM) landed across the globe [5]. In Colombia, four decades of civil war have left more than 100 thousand antipersonnel (AP) mines landed across 422 municipalities (40% of the national territory). These mines cause approximately 150 deaths per year, which a 31% are children [6]. These mines are American and Belgian, as well as mines that were made for the National Military Industry INDUMIL. However, a considerable amount was made in an artisan way by the guerrillas (*e.g.*, FARC and ELN[1]) . These last ones are called improvised explosive devises (IEDs), and are the principal problem in Colombian demining activities, due to their non-metallic content. In recent years, serious efforts for developing technologies that can help in landmine detection have been done [7]. Among these technologies, a great importance is given to the GPR because of the ability to detect metallic and low-metallic AP landmines by non-invasive subsurface sensing. Still, its main drawback is the complex nature of its data, and then their interpretation is usually limited in defining general "areas of interest" instead of accurately determining the shape and position of the target.

In this study, two-dimensional data-sets (B-scans) from a commercial time-domain GPR (800 MHz) are analyzed in order to extract relevant information. These data-sets are collected in different scenarios. In Section II, a description of the targets and the measurements setup are given. In order to achieve optimal separation of the target signatures from the background, the problem is viewed as an image-processing one as the collected two-dimensional data-sets represent image segments. Section III is devoted to the denoising techniques used to remove unwanted reflections and to extract relevant pieces of information as target position and depth, and the dielectric permittivity (real part) of the soil. Migration theory is then applied for focusing the scattered signals back in their point of origin. The Stolt migration is used and is introduced in Section IV. The analysis of the migrated data is presented in Section V. Finally, Section VI concludes our study.

2 Measurement Setup

The data are acquired at the test land of the Military School of Engineering, Colombia, for sandy and loamy soils (see Fig. 1). In this study we focus on the signatures of two types of

1. Fuerzas Armadas Revolucionareias de Colombia - FARC, Ejercito de Liberacion Nacional - ELN

FIG. 1: Test land at the Military School of Engineering, Colombia

AP mines: a Colombian AP mine and an improvised explosive devise made by the guerrillas. In the remainder of this paper these mine types will be referred to as APM A and B respectively. AP mine A has a plastic casing and low metallic content. AP mine B has a plastic casing and non-metallic content. Their dimensions, burial depths (from the top of the mine), and distance (from a reference point to the middle of the mine along the scanning direction) are summarized in Table 1.

For the acquisition we used a monostatic radar system in the time-domain developed by the Mala GeoScience Group [2], with a 800MHz antenna and a repetition frequency of 100kHz. All data have been recorded using a 10 ns time window of 512 samples corresponding to a time sampling interval of approximately 20ps. The resolution of each sample point is 16 bit. The data have been acquired along one surface direction and the antenna system was positioned above the soil surface. The distance was measured by an incremental encoder connected to the system and the antenna was moved whit a constant velocity. In Fig. 2, the collected data for the loamy soil is represented in function of the scanning distance and the time-of-flight of the signal (time to reach the reflection point and to come back to the receiver antenna) for the two types of mines.

TAB. 1: *Target features**

Target	Dimension (m)	Depth (m)	Distance (m)
APM A	d:0.075, h:0.07	0.01	0.60 (l), 0.60 (s)
APM B	d:0.120, h:0.07	0.10	0.60 (l), 0.60 (s)

* d: diameter, h: height, (l): loamy soil, (s): sandy soil

3 Ground Clutter Subtraction

To eliminate the clutter from an image we have first to define it. The electromagnetic waves transmitted by the radar are propagated through the air and, of course, to the ground. At any interface between any two media having different electromagnetic properties, part of the electromagnetic energy is reflected backwards to the receiver and a part is transmitted into the second media. The same phenomenon occurs when the transmitted signal comes across a buried object (of which electromagnetic parameters differ from those of the ground) and, unfortunately, across any other non-uniformities inside the ground (stones, layers having different electromagnetic parameters, etc). All these reflections which are not related to the object's own scattered field are called clutter [8].

Two denoising methods are used to filter the ground clutter level. These methods are implemented by convolving the image with a horizontal high pass filter. The derivative of a Gaussian represents such a filter. It is important to notice that the window width of the filter is crucial for the final result. The choice of the filter length depends on the size and resolution of the image. Several tests show that a too small window introduces noise, and a large window minimizes the contrast of the image [3]. We achieved the best results with a 10-pixels wide filter. Every change in the image resolution or image size needs a reevaluation of the ideal filter width. Note that a vertical noise was introduced to the image (because horizontal filtering is a derivative action). To reduce this effect, a vertical 1x5-pixels filter was created by a Gaussian function. This filter is used to average over 5 pixels in order to reduce the noise in the vertical direction. Once the image is filtered, we can see the hyperbolic response of the target. An algorithm to detect curves is applied for extracting relevant information from the equation of the hyperbola. The Randomized Hough Transform is used [3]. RHT randomly selects n pixels from an image and fits them to a parameterized curve. If the pixels fit within a tolerance, they are added to an accumulator with a score. Once a specified number of pixel sets are selected, the curve with the best score is selected from the accumulator and its parameters are used to represent a curve in the image. In RHT, if a curve in the accumulator is similar to the curves being tested, the parameters of the curves are averaged together and the new average curve replaces the curve in the accumulator. The extracted information form the hyperbola equation in included in the migration algorithm.

4 Phase-shift Migration

Phase-shift migration was first applied for seismic imaging by Stolt in 1978 [9]. The principle has been adopted for satellite SAR processing [10] and it has also been widely utilized for processing of GPR data in two dimensions [11]. Phase-shift migration is based on a transformation from the frequency domain ω to the wavenumber domain k. Consider the raw data set $b(x, z, t)$ collected from the radar, x being the B-scan distance, z the depth, and t the time-of-flight. Applying a 2D Fourier transform with respect to the spatial distance x and the time t to spatial frequency k_x, the result is an unfocused wavenumber data set

$$B(k_x, z, \omega) = \int\int b(x, z, t) e^{ik_x x - i\omega t} \mathrm{d}x\mathrm{d}t. \qquad (1)$$

The Fourier transformation along the x coordinate only makes sense if the propagation velocity does not vary in this direction. The method allows variations of the propagation velocity in the z direction. Defining the wavenumber vector k as the vector sum of k_x and k_z for one-way propagation, we have:

$$k = |\mathbf{k}| = \sqrt{k_x^2 + k_z^2} = \frac{\omega}{\upsilon} = \frac{2\pi}{\lambda}, \qquad (2)$$

2. http://www.malags.se

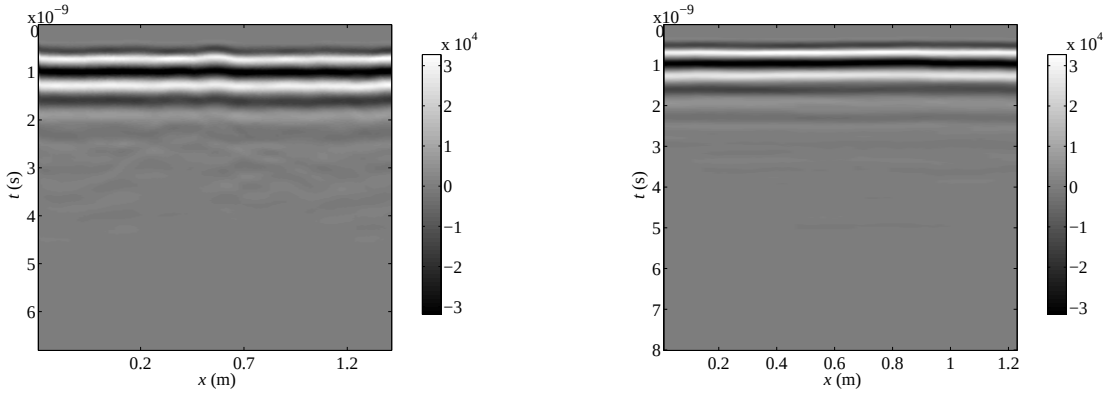

FIG. 2: *B-scans on loamy soil for APM A (a) and B (b).*

where υ is the propagation velocity of the ground ($\upsilon = c/\sqrt{\varepsilon_r}$, being ε_r the relative dielectric permittivity, extracted from the equation of the hyperbola) and λ is the wavelength in the ground. The direction of the **k**-vector is identical to the traveling direction of a plane wave propagating from the target to the antenna. Assuming only upward coming waves, and by introducing k_z from (2) in (1), the Fourier transform of the wavefront at depth z is done by

$$B(k_x, z, \omega) = B(k_x, 0, \omega)e^{-ik_z z}. \quad (3)$$

The migrated data will be the inverse Fourier transform of (3) at time t=0:

$$\widehat{b}(x, z) = b(x, z, 0) = \int\int B(k_x, 0, \omega)e^{-i(k_x x + k_z z)}\mathrm{d}k_x\mathrm{d}\omega. \quad (4)$$

Equation (4) is the general representation of the phase-shift migration. The implementation of this method is computationally intensive, because of the number of floating point operations needed for migration [2]. For the reduction of the calculation time, a variant of the phase-shift migration for a constant propagation velocity is used. This variant was developed in [9]. In the special case where $\upsilon(z)$ is constant, (4) can be further developed by changing the variable $\mathrm{d}\omega$ to $\mathrm{d}k_z$. By replacing $\mathrm{d}\omega$ from (2), the data must be scaled by the Jacobian of the transformation from ω to k_z, $\frac{k_z \upsilon^2}{\omega}$. Hence, for the Stolt migration, (4) becomes

$$\widehat{b}(x, z) = \upsilon^2 \int\int \frac{k_z}{\omega} B(k_x, 0, \omega)e^{-i(k_x x + k_z z)}\mathrm{d}k_x\mathrm{d}k_z. \quad (5)$$

5 Results and Discussions

In Fig 2, the B-scans on loamy soil for AP mine A and B are shown. The reflection of the buried object is completely drowned in the ground reflection (between 0.5 ns and 1.5 ns). By applying denoising and segmentation techniques, relevant information can be extracted for the data. It is summarized in Table 2. It can be seen that the extracted values are quite close to real ones. The differences between the real values and the calculated ones are due to the three-dimensional form of the APM. The depth and distance were measured respectively from the top and from the middle of the mine. However, the backscattered signal received by the antenna comes from different points over the surface of the mine [2], and then different hyperbolas will be appear in the B-scan. By averaging these different hyperbolas, we will find a very good approximation of the position of the mine, but not the exact one.

TAB. 2: *Calculated depth and distance**

Target	Depth (m)	Distance (m)
APM A	0.0078	0.671 (l), 0.624 (s)
APM B	0.1056	0.652 (l), 0.636 (s)

* (l): loamy soil, (s): sandy soil

In Fig 3, results of applying the migration algorithm for the denoised data are shown. From this figure, the shape of the target on the B-scan direction can be seen. For the APM A, it appears at 0.5 ns. This points out that the AP mine is placed at the soil surface. For the AP mine B, it appears at 1.0 ns. This points out that the mine is buried close to the surface ($\sim$ 10 cm). Over the scanning axis, the position of the target (the shape of the target) appears quite close to the calculated and real position of the target in the soil.

6 Conclusions

In this paper, denoising and migration methods have been applied on real GPR data. The data are collected in two types of soil and for conventional and non-conventional APM. Namely, the major limit factor to detect APM with GPR is the ground clutter. To reduce the ground clutter an horizontal filtering is applied. Since the buried object signature on GPR 2D data are represented by a hyperbolic shape, the RHT is applied for the isolation of the object response. The relevant pieces of information that have been extracted from the equation of the hyperbola give us a very good approximation of the position of the buried object. The size of the object can be deduced from the migrated data. All this information can be used in data fusion architectures, involving other sensor data. The performance of these algorithms on real GPR data is encouraging. These algorithms are not computationally intensive. However, it depends on the

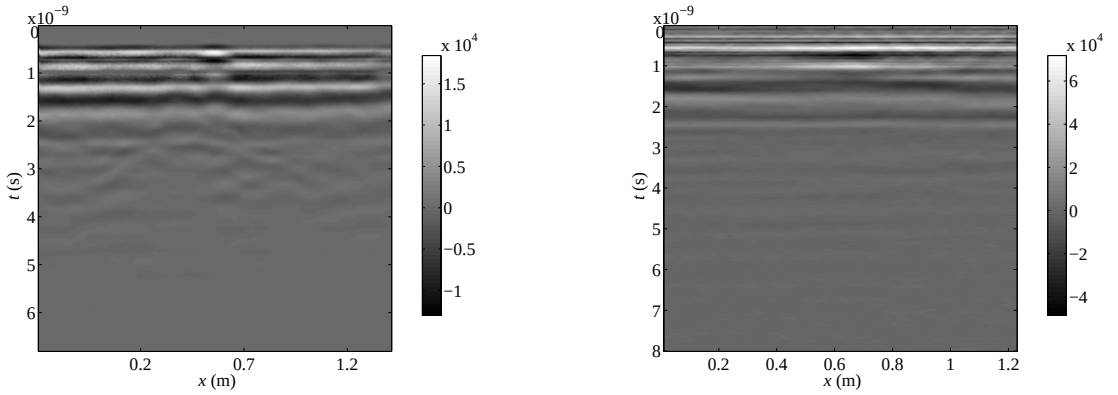

FIG. 3: *Results of applying denoising and migration techniques for B-scans on loamy soil for APM A (a) and B (b).*

size of the database. In order to make an objective analysis, the overall processing still needs to be validated in different conditions and for more than one object buried in the soil.

Acknowledgment

This research project is carried out at the Signal and Image Centre of the Royal Military Academy, Belgium, and at the Department of Electrical and Electronic Engineering of the University of Los Andes, Colombia, in collaboration with the Telecommunications Laboratory, Catholic University of Louvain, Belgium. It is supported by a research grant funded by the Ministry of Defence of Belgium, in the scope of the BEMAT project, and by a research grant from Colciencias (Colombian Institute for the Development of Science and Technology, Colombia). The authors would like to thank the Colombian Military Forces for their support, specially the personnel of the MARTE group and the BAMAI laboratory.

Références

[1] N. Milisavljevic, "Analysis and fusion using belief functions theory of multisensor data for close-range humanitarian mine detection," Ph.D. dissertation, Ecole Nationale Superieure des Telecommunications, France - Royal Military Academy, Belgium, 2001.

[2] B. Scheers, "Ultra-wideband ground penetrating radar with application to the detection of anti personnel landmines," Ph.D. dissertation, Catholic University of Louvain - Royal Military Academy, Belgium, 2001.

[3] O. Lopera, N. Milisavljevic, B. Macq, I. van den Bosch, S. Lambot, and A. Gauthier, "Analysis of segmentation techniques for landmine signature extraction from Ground Penetrating Radar 2D data," in *eProceedings of the II International IEEE Andean Region Conference, ISBN 958-33-6534-3*, IEEE, Ed., Bogota, Colombia, 2004.

[4] O. Lopera, S. Lambot, N. Milisavljevic, B. Scheers, and I. van den Bosch, "Background subtraction in the frequency domain for focusing ground-penetrating radar data," *Near Surface Geophysics*, vol. Special Issue, p. Submitted, 2005.

[5] GICHD, *A guide to Mine Action*. Geneva: GICHD., 2003.

[6] Human Rights Watch, *Landmine Monitor Report 2002, Toward a Mine-free World*. Whashington D.C.: ICBL, 2002.

[7] J. MacDonald, J. Loockwood, T. Altshuler, T. Broach, L. Carin, R. Harmon, C. Rappaport, W. Scott, and R. Weaver, *Alternatives for Landmine Detection*. USA: RAND, 2003.

[8] A. Yarovoy, V. Kovalenko, and A. Fogar, "Impact of clutter on buried object detection by Ground Penetrating Radar," in *International Geoscience and Remote Sensing Symposium*, France, 2003.

[9] R. Stolt, "Migration by fourier transform," *Geophysics*, vol. 43, pp. 23–48, 1978.

[10] C. Cafforio, C. Prati, and E. Rocca, "SAR data focusing using seismic migration techniques," *IEEE Trans. Aeroespace and Electronic Systems*, vol. 27, pp. 197–206, 1991.

[11] H. Yu, X. Ying, and Y. Shi, "The use of FK-techniques in GPR processing," in *6th International Conference on Ground Penetrating Radar*, Sendai, Japan, 1996, pp. 595–600.